IEEE Access
Multidisciplinary | Rapid Review | Open Access Journal

Received May 1, 2020, accepted May 28, 2020, date of publication June 1, 2020, date of current version June 10, 2020.

Digital Object Identifier 10.1109/ACCESS.2020.2999206

Weighted ABG: A General Framework for Optimal Combination of ABG Path-Loss Propagation Models

DAVID CASILLAS-PEREZ, CARLOS CAMACHO-GÓMEZ, SILVIA JIMÉNEZ-FERNANDEZ, JOSE A. PORTILLA-FIGUERAS, AND SANCHO SALCEDO-SANZ

Department of Signal Processing and Communications, Escuela Politécnica Superior, Universidad de Alcalá, 28805 Alcalá de Henares, Spain

Corresponding author: Sancho Salcedo-Sanz (sancho.salcedo@uah.es)

This work was supported by the Universidad de Alcalá - ISDEFE Chair of Research in ICT and Digital Progress.

ABSTRACT In this paper we propose a novel path-loss model, the *Weighted ABG* (WABG), which suitably allows integrating or combine different available datasets, or previously proposed 5G propagation path-loss models from the state-of-the-art. Our proposal is therefore a new ABG-based approach which integrates other existing models, leading to the best possible approximation in least-square sense, considering different weighting policies. We evaluate the performance of the WABG in several 5G scenarios, and we carry out a complete comparison of the proposed method against several recently published ABG models, showing that the WABG obtains the best results in terms of model's accuracy.

INDEX TERMS 5G, path-loss, mmWave, ABG propagation models, models combination.

I. INTRODUCTION

The fifth generation of mobile communications systems (5G) will bring along a complete revolution in applications and experiences [1]. Many sectors such as health, industry, vehicles, videogames or business, among many others, will completely change thanks to this technology. Characteristics of the new mobile network include a 10 Gbps downlink throughput, 1 ms latency, 99.999% reliability and a large number of devices connected simultaneously to the access network [2], [3].

Wirelessly providing these high data rates and quality parameters demands new innovative technologies, not implemented in the fourth generation of mobile communications (4G), such as, massive multiple-input multiple-output (mMIMO) [4]–[6] or non-orthogonal multiple access (NOMA) [7]–[9]. However, even with these new techniques, the frequency bands where legacy mobile communication systems are placed will not fulfill the requirements of the 5G technology. This is the reason why the Third Generation Partnership Project (3GPP [3]) has pointed out the need to use mmWave frequency bands for hosting future 5G services [10].

Among the different issues related to the use of mmWave frequencies, the extremely high path-loss occurring at these frequencies is a major technological issue [11]–[13]. Like in previous generations, radio propagation has been a key aspect on mobile communications design. Propagation models are used to estimate the path loss and, consequently, to determine the maximum coverage range of a given radio base station. Generally speaking, there are three types of radio propagation models [14]: ray tracing or optical models [15], [16], dominant path models [17] and statistical models [18]–[20]. *Ray tracing-optical models* are based on the addition of the individual contribution of multiple rays. These models require specifying the area under study including geographic information (buildings, streets, elevations), as well as building construction materials, in order to calculate the scattering, reflection and diffraction for each individual ray. Consequently, the ray-tracing models present a high computational cost, and need to be implemented on large simulators. *Dominant path models* only consider the main contributing ray between the transmitter and receiver, and specific information regarding the area and the environment's materials [21]. They reduce the computational cost compared with the ray-tracing

The associate editor coordinating the review of this manuscript and approving it for publication was Zesong Fei.

models, but also require the area's materials database. Finally, *statistical models* (aka empirical models) provide fair estimations of the propagation path-losses by using few environment parameters, therefore they present a very low computational cost. The statistical strategy establishes an optimization problem based on different statistic criteria, such as, Maximum Likelihood (ML), Maximum a Posterior (MAP) criteria or Least-Squares (LS), and looks for the model which best adjusts the path-loss samples in this sense. In fact, radio propagation models implement mathematical formulation, which depending on the model's complexity, may be used for either site specific and/or general site calculations [22]. These models are very useful when the available area information is reduced or when the computation time requirements are limited, for instance, in the estimation of the maximum cell range around the 360° directions (note that in ray-tracing only one direction is obtained).

Focusing on the statistic models, several studies propose the use of different propagation path-loss models in 5G systems [3], [12], [18], [19], [23]–[26]. However, the large-scale path-loss propagation model named the Alpha-Beta-Gamma (ABG) model [3], [12], [19] is currently the most used path-loss model in 5G applications, and it is also the model established by the 3GPP as the standard model for 5G [3]. There are specific ABG models for different 5G scenarios, such as, Urban Micro and Macro cells (UMi and UMa, respectively), in different environments such as Line-of-Sight (LOS) and Non-Line-of-Sight (NLOS). The implementations of these models cover a wide working range of distances and frequencies, many of which overlap in terms of distance or frequency [12], [19]. To name some examples, [27] studied the wideband channels at 9.6, 28.8 and 57.6 GHz in LOS and NLOS. In [28], [29] a measurement campaign and path-loss modeling was carried out in the 60 GHz band. And in [30] Aalto University studied frequencies in the E-band, specifically the 71 to 76 GHz and the 81 to 86 GHz bands. Although all of these models estimate similar path-loss values, especially in LOS (where propagation path-loss modelling is close to the free-space modeling), dissimilarities occur, and policies for balancing the path-loss approaches are needed to create an integral model.

In the literature, there are not many integral approaches that deal with the existent ABG models and cover all the established distance-frequency ranges in 5G. The most recent approach in [19] proposes to create a database by combining different 5G path-loss databases. This new database leads to a new set of ABG coefficients and, therefore, we have named this procedure as the *basic and integrated* ABG model. To construct the new ABG model, a large dataset is needed to lead to reliable ABG coefficients. Nevertheless, the first issue of this approach is that merging is done without a balancing or weighting policy. All input models weight the same when creating the integrated (output) model, regardless of their accuracy. Hence, tending to overestimate those models made with a larger number of samples. The second issue is that, in order to create the new database, it requires that all input models are defined similarly (i.e. input models are defined by a path-loss dataset). This is, in general, an extremely hard requirement since we do not often count on public databases. Many published studies (summarized in [19]) only provide the resulting ABG coefficients of a model, its ranges and a noise figure indicating how accurate the model is with respect to its database.

Input models and/or the provided raw path-loss datasets may cover different frequency or distance ranges, may be defined using ABG coefficients or field measurements, may have a larger or a smaller number of points, etc. Therefore, it is paramount to address correctly the importance of the former baseline models.

The main objective of the present paper is to obtain a single (output) ABG-based model that is able to combine different (input) ABG models and/or (input) raw path-loss datasets provided by different studies. To perform the integration, the novelty of this research is that these inputs are weighted using a balancing policy that allows to surpass the aforementioned drawbacks of the state-of-the-art approaches. In this research, this model is named as Weighted ABG (WABG), and its main characteristic is that it preserves the low number of parameters characteristic to the ABG models. Figure 1 shows an illustrative flowchart of our proposal.

We have tested the WABG in several 5G scenarios, including UMi and UMa scenarios, in both LOS and NLOS environments. We also compare the proposed WABG model with several recently published alternative ABG models, including the basic integrated ABG model, in the different 5G scenarios considered, obtaining excellent results in terms of path-loss standard deviation.

The remainder of the paper is structured as follows: Section II reviews the theoretical aspects of the ABG propagation model. Section III describes in detail the proposed WABG model, including the weighting policies which can be applied to generate it. Section IV first shows an instructive example of how to build a WABG model from the beginning, then it details an study of the effect of the different weightings, and finally it presents a complete set of experiments in LOS and NLOS environments for the different 5G considered scenarios. This section also shows a direct comparison with the state-of-the-art ABG models. Section V closes the paper with some final conclusions and remarks.

II. THE ABG MODEL

The Alpha Beta Gamma (ABG) model [3] is a large-scale path-loss propagation model for all generic frequencies. The model is not highly constrained, so it is frequently used for specific scenarios, distinguishing LOS and NLOS environments; or finding specifically calculated ABG model for different 5G scenarios, such as UMi and its variants (UMi Street Canyon, UMiSC, and UMi Open Square, UMiOS) and UMa. In NLOS, for instance, generally ABG models divide the distance range in different partitions to gain accuracy in specific applications [3].

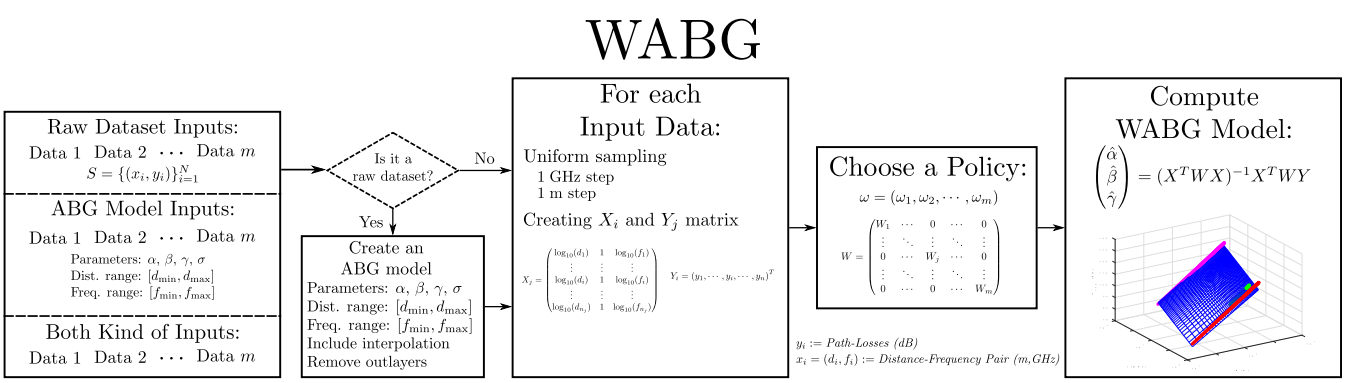

FIGURE 1. **WABG Flowchart. The proposed WABG is an ABG-based model which integrates raw datasets and/or other ABG models from different studies using a weighting policy.**

The ABG models calculate the path-loss as follows:

$$P_{\text{ABG}}(d,f)[\text{dB}] = 10\alpha \log_{10}(d) + \beta + 10\gamma \log_{10}(f) + \xi, \tag{1}$$

where P_{ABG} is the path-loss in decibels (dB) logarithmically dependent on the distance d and frequency f, measure in meters (m) and Gigahertz (GHz) respectively. The involved distance d is the Euclidean 3D distance between the transmitter and the receiver, and the frequency f refers to the carrier frequency. The coefficients α, β, γ define the ABG model. Specifically, α and γ are the coefficients related to the log-distance and log-frequency respectively, and β is an offset term. They all define a plane in the 3D space where the path-loss, log-distance and log-frequency form the Cartesian axes. The random variable ξ models the large-scale signal fluctuation produced along the transmissions. A particular statistical distribution for the noise ξ is not assumed, but a zero mean and a finite variance σ^2 is required.

The ABG model discovers the α, β and γ values by setting an ordinary linear least-squares problem, which consists of adjusting the coefficients to those which fit the best to a data set [19]. Let $D = \{(x_i, y_i) \mid 1 \leq i \leq n\}$ be the set of n available pairs of input-output observations, where $x_i = (d_i, f_i)$ is an input pair of distance-frequency, also referred as the independent variable; and y_i its corresponding path-loss measure, the dependent variable. The established ABG model relates x_i and y_i by the Equation (1). The fit of a model to a data point (x_i, y_i) is measured by its residual, defined as the difference between the measured path-loss and the value predicted by the ABG model:

$$r_i = y_i - P_{\text{ABG}}(d_i, f_i). \tag{2}$$

The optimal parameter values are obtained by minimizing the sum of the squared residuals R:

$$R = \sum_{i=1}^{n} r_i^2 = \sum_{i=1}^{n} \left(y_i - P_{\text{ABG}}(d_i, f_i)\right)^2. \tag{3}$$

Just for linear models, which is the case of the ABG (see Equation (1)) there exist a unique solution to the problem of finding the best parameters $(\hat{\alpha}, \hat{\beta}, \hat{\gamma})$ with following closed-form expression:

$$\begin{pmatrix}\hat{\alpha}\\ \hat{\beta}\\ \hat{\gamma}\end{pmatrix} = (X^T X)^{-1} X^T Y, \tag{4}$$

where X is a matrix whose ijth-element is the ith-observation of the jth independent variable:

$$X = \begin{pmatrix} \log_{10}(d_1) & 1 & \log_{10}(f_1) \\ \vdots & \vdots & \vdots \\ \log_{10}(d_i) & 1 & \log_{10}(f_i) \\ \vdots & \vdots & \vdots \\ \log_{10}(d_n) & 1 & \log_{10}(f_n) \end{pmatrix} \tag{5}$$

and $Y = (y_1, \cdots, y_i, \cdots, y_n)^T$ its corresponding path-loss vector whose ith-element is the path-loss of the ith-observation. Note that $(X^T X)^{-1} X^T$ is the Moore-Penrose inverse of X. The Gauss-Markov theorem guarantees that the obtained linear regressor is the Best Linear Unbiased Estimator (BLUE), in terms of minimum variance. The following assumptions concerning the set of error random variables $\{\xi_i \mid 1 \leq i \leq n\}$ have been taken:

1) The noise variables ξ_i are zero mean: $\text{E}[\xi_i] = 0$.
2) They are *homoscedastic*, that is, all they have the same finite variance $\text{Var}[\xi_i] = \sigma^2 < \infty$.
3) Distinct error terms are uncorrelated $\text{Cov}[\xi_i, \xi_j] = 0\ ,\ \forall i \neq j$.

The ABG model can manage a single carrier frequency by fixing its γ coefficient to 0 or 2 [18], [20], [31], becoming a two-parameters model (α and β). The mathematical treatment to obtain the best coefficients $(\hat{\alpha}, \hat{\beta})$ is similar to the one shown above.

III. PROPOSED WEIGHTED ABG MODEL

Multiple ABG coefficients for the different state-of-the-art path-loss databases can been obtained for several 5G scenarios. Particularized for a single carrier frequency or a near band of carrier frequencies, ABG models have shown in general good accuracy, especially when they are computed from one

specific database. However, ABG models computed from multiple databases, with different distance-frequency ranges, do not achieve such accurate results: Most of them collect all data from the multiple state-of-the-art datasets to create a larger one, obtaining the best parameters following the steps of the previous Section II (see [19]). These integrated models do not contemplate unbalanced data from the different database or the residual values associated with each range of distance or frequencies. In addition, note that assuming the homoscedastic preservation along the different distance-frequency ranges leads to inaccurate and unbalance integrated models.

In order to improve these previous issues with integrated ABG models, we propose a weighted model which considers the *heteroscedastic* property along the different data from the dataset for managing multiple range of distances and frequencies. The proposed Weighted ABG model (WABG), which surpasses the mentioned inconveniences of integrated path-loss approaches, is following defined.

We observe three main scenarios or cases for proposing the WABG path-loss model:

1) The first scenario is defined by a family of propagation path-loss datasets $\{S_j \mid 1 \leq j \leq m\}$. Each dataset S_j contains a set of input-output observations $S_j = \{(x_i, y_i) \mid 1 \leq i \leq n_j\}$ in its corresponding range of distances and frequencies. Some of them may contain significant distance or frequency gaps which may need to be filled using interpolation algorithms. Usually the different datasets contain observations from a single carrier frequencies or a near frequency band, which leads to very accurate individual ABG models. Consequently, each dataset S_j has associated its own ABG model defined by its parameters $\text{ABG}(S_j) = (\alpha_j, \beta_j, \gamma_j)$, computed following the steps of Section II. Associated with the ABG model, the standard deviation of the error σ can be easily calculated, once the optimal ABG model is obtained, by applying Equation (6):
$$\sigma_j = \sqrt{\frac{R_j}{n_j}} = \sqrt{\frac{\sum_{i=1}^{n_j} \left(y_i - P_{\text{ABG}}(d_i, f_i)\right)^2}{n_j}} \tag{6}$$
Note that the standard deviation σ_j expressed in Equation (6) determines the model's quality.
2) The second scenario for defining the WABG, is the case where we do not have access to the complete databases, but only to the already calculated ABG coefficients $\{(\alpha_j, \beta_j, \gamma_j) = \text{ABG}(S_j) \mid 1 \leq j \leq m\}$ and its corresponding standard deviation σ_j valid for a specific distance-frequency range. This scenario corresponds, for example, to a case where the employed datasets are not public.
3) The third scenario is a mixture of the two previous ones, the general case, where we can have measurements for some distances and frequencies and also ABG coefficients for other, and we would like to collect all this information into a new integrated ABG path-model.

In any of these scenarios, the proposed WABG model works by integrating (combining) several ABG models for different ranges of distances and frequencies. Thus, after obtaining the ABG model and its associated standard deviation in the case of scenario 1, directly from the given models in scenario 2, or a mixture of both in scenario 3, we create a synthetic dataset $\tilde{S}_j$ for each corresponding ABG model, and form a collection of observation datasets $\{\tilde{S}_j \mid 1 \leq j \leq m\}$. In order to do this, we equally vary the distance and frequency covering all the range of each given ABG model, and annotate the associated standard deviation. As a practical rule, we vary distances and frequencies in steps of 1 m and 1 GHz respectively. In case of ABG models computed for a single frequency, we only vary the distance in its corresponding range.

At the end of this process, we have m simulated databases with observations $\tilde{S}_j = \{(x_i^j, y_i^j) \mid 1 \leq i \leq n_j\}$, which belong to a specific model and have the same standard deviation σ_j. Observations from different databases may have different standard deviations, therefore, collecting all the observations in a unique set and calculating an ABG model leads to wrong path-loss estimations (such as the basic integrated ABG model). WABG manages these variability of the deviations, avoiding this important issue to construct a robust integrated model.

The WABG establishes a weighted least-squares problem, a special case of generalized least-squares. It occurs when all the off-diagonal entries of the correlation matrix of the residuals are zero. The variances of the observations, which are the unique non-null elements placed along the covariance matrix diagonal, may still be unequal. It is the so-called *heteroscedasticity* property which differs from the basic integrated ABG models. In WABG, the optimal parameter values are obtained by minimizing a weighted sum of squared residuals, which involves the heterogeneous variance of the observations:
$$S = \sum_{i=1}^{n} W_{ii} r_i^2 = \sum_{i=1}^{n} W_{ii} \left(y_i - P_{\text{ABG}}(d_i, f_i)\right)^2, \tag{7}$$
where W is the inverse of the correlation matrix, see Equation (8).
$$W = \begin{pmatrix} \frac{1}{\sigma_1^2} & \cdots & 0 & \cdots & 0 \\ \vdots & \ddots & \vdots & \ddots & \vdots \\ 0 & \cdots & \frac{1}{\sigma_i^2} & \cdots & 0 \\ \vdots & \ddots & \vdots & \ddots & \vdots \\ 0 & \cdots & 0 & \cdots & \frac{1}{\sigma_n^2} \end{pmatrix} \tag{8}$$
Aitaken [32] proved that the coefficients calculated in this way $(\hat{\alpha}, \hat{\beta}, \hat{\gamma})$ are the BLUE if each weight is equal to the reciprocal of the variance of the measurement, see Equation (7), and provides the following closed-form

solution:

$$\begin{pmatrix}\hat{\alpha}\\ \hat{\beta}\\ \hat{\gamma}\end{pmatrix} = (X^T W X)^{-1} X^T W Y. \tag{9}$$

where X is a matrix whose ijth-element is the ith-observation of the jth independent variable, and W is represented in Equation (8). Observe how the computation complexity to solve Equation (9) is reduced to invert matrix $X^T WX$, similarly to the ABG models, where complexity is reduced to invert $X^T X$.

Particularized for our WABG model, X is a block matrix defined by stacking all the observations of the different databases $\tilde{S}_j$:

$$X = \begin{pmatrix} X_1 \\ \vdots \\ X_j \\ \vdots \\ X_m \end{pmatrix}, \quad X_j = \begin{pmatrix} \log_{10}(d_1) & 1 & \log_{10}(f_1) \\ \vdots & \vdots & \vdots \\ \log_{10}(d_i) & 1 & \log_{10}(f_i) \\ \vdots & \vdots & \vdots \\ \log_{10}(d_{n_j}) & 1 & \log_{10}(f_{n_j}) \end{pmatrix}. \tag{10}$$

Note that the block X_j that corresponded to an ABG model valid for a single frequency has its third column constant. The inverse of the correlation matrix W is also a partitioned matrix, where the observations that belong to the same dataset S_j have the same variance, as we expressed in Equation (11).

$$W = \begin{pmatrix} W_1 & \cdots & 0 & \cdots & 0 \\ \vdots & \ddots & \vdots & \ddots & \vdots \\ 0 & \cdots & W_j & \cdots & 0 \\ \vdots & \ddots & \vdots & \ddots & \vdots \\ 0 & \cdots & 0 & \cdots & W_m \end{pmatrix},$$

$$W_j = \begin{pmatrix} \frac{1}{\sigma_j^2} & \cdots & 0 & \cdots & 0 \\ \vdots & \ddots & \vdots & \ddots & \vdots \\ 0 & \cdots & \frac{1}{\sigma_j^2} & \cdots & 0 \\ \vdots & \ddots & \vdots & \ddots & \vdots \\ 0 & \cdots & 0 & \cdots & \frac{1}{\sigma_j^2} \end{pmatrix}_{n_j \times n_j} \tag{11}$$

Now the corresponding standard deviation, considering the weighting, is computed as depicted in Equation (12).

$$\sigma = \sqrt{\frac{\sum_{i=1}^{N} W_{ii} r_i^2}{\sum_{i=1}^{N} W_{ii}}} = \sqrt{\frac{\sum_{i=1}^{N} W_{ii} \left(y_i - P_{\mathrm{ABG}}(d_i, f_i)\right)^2}{\sum_{i=1}^{N} W_{ii}}}. \tag{12}$$

We will see in the next section different policies to form the inverse of the correlation matrix W in order to correctly balance the WABG model, attending to different criteria. As the inverse of the correlation matrix W is diagonal, it can be expressed through the so-called weighting vector ω.

A. WEIGHTING POLICIES

We propose three main policies of weightings applied to the WABG model when it is built by integrating several ABG models from different datasets:

1) Equalizing by the Number of Points: The ABG models integrated by the WABG may cover different range of distance and frequencies, and be built from datasets with different number of points. Each ABG model given for computing a WABG should be considered with the same importance independently of the number of points that were used to create them. Consequently, equalizing the WABG providing same grade of importance requires the following weighting vector:

$$\omega_{\mathrm{N}} = M \left(\overbrace{\frac{1}{n_1}}^{n_1 \text{times}}, \cdots, \overbrace{\frac{1}{n_i}}^{n_i \text{times}}, \cdots, \overbrace{\frac{1}{n_m}}^{n_m \text{times}} \right), \tag{13}$$

where n_i is the number of points using in each model and M is the least common multiple of the set $\{n_i \mid 1 \leq i \leq n\}$.

2) Weighting by the Standard Deviation: The initial ABG models used to create the WABG may have different standard deviation which should be consider to weight. ABG models with large standard deviation should have less weighting than others with a small one. A good weight vector ω for the WABG uses the inverse of the standard deviation as follows:

$$\omega_{\sigma} = \left(\overbrace{\frac{1}{\sigma_1^2}}^{n_1 \text{times}}, \cdots, \overbrace{\frac{1}{\sigma_i^2}}^{n_i \text{times}}, \cdots, \overbrace{\frac{1}{\sigma_m^2}}^{n_m \text{times}} \right) \tag{14}$$

3) Mixture of the previous policies: Computing the Hadamard product of both vectors:

$$\omega = \omega_N \odot \omega_{\sigma} \tag{15}$$

The corresponding weighting matrix W is a matrix whose diagonal matches its weighting vector ω. Note that using a weighting vector of ones $\omega = (1, \cdots, 1)$, the obtained WABG model becomes an ABG whose weighting matrix is the identity $W = I$.

IV. COMPUTATIONAL EXPERIMENTS AND RESULTS

In this section, we compare the WABG model with the state-of-the-art ABG models computed from several 5G datasets, specifically, from those one provided by the companies Nokia, Qualcomm, and the Universities of Aalborg (AAU), New York (NYU) and Aalto (ALU). We distinguish between three different kinds of 5G scenarios: Urban Micro-cellular Street Canyon (UMiSC), Urban Micro-cellular Open Street (UMiOS) and Urban Macro-cellular (UMa). We also distinguish between two different 5G environments: LOS and NLOS. The LOS environment presents lower standard deviation σ compared to the NLOS cases, a consequence of the non-existence of a direct Line-of-Sight.

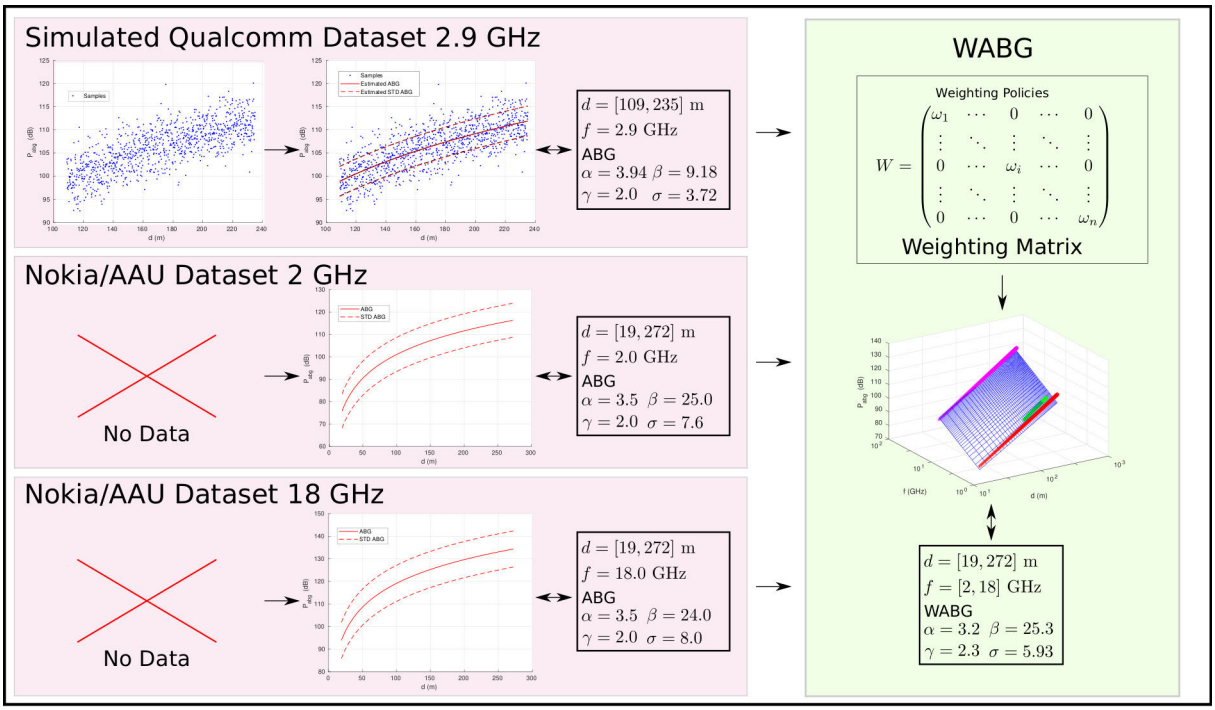

FIGURE 2. Example of WABG construction. A low band WABG is developed in the distance range from 19 to 272 m and frequency range from 2 to 18 GHz. ABG models of both Nokia/AAU datasets [30] at 2.9 and 18 GHz are given as input models. Simulated points of the Qualcomm dataset [19] at 2.9 GHz are also considered.

The ABG models for each 5G scenario in the NLOS environment have been obtained from [19]. The corresponding ABG models for each 5G in LOS were computed from the works published in [11], [12]. According to this, we will provide a WABG model covering a wide range of frequencies. In NLOS, where the number of available models is high, we will also provide a model for low and high frequencies. The division between low and high frequencies was established by the state-of-the-art methods [11], [12]. Consequently, we have followed this division to allow comparison among them. Note that this division is not a requirement of the proposed model and we can design a WABG model in any other frequency range.

Moreover, the metric error used is the weighting standard deviation σ, as expressed in Equation (12). Note that the weighting standard deviation directly leads to the standard deviation assuming as weighting matrix the identity $W = I$.

This section is then structured into three subsections: we first give an end-to-end real computation example of a WABG departing from both ABG models and datasets, the mixture scenario (see Section III). Then, we analyze and compare the proposed weighting policies of Section III-A. Finally, we give the WABG coefficients in LOS and NLOS for the studied 5G scenarios UMiSC, UMiOS and UMa, and we carry out a comparison with the available large-scale propagation path-loss models in the literature.

A. REAL WABG COMPUTATION EXAMPLE

This section presents the calculation of the WABG model in the third scenario, the most general scenario as it includes the first and second scenarios (all of them described in Section III). Figure 2 shows an example of the construction of the WABG model in this case.

We have elaborated a low band WABG model using three different datasets corresponding to the 5G UMiSC scenario in NLOS environment. These three models correspond to the first three rows presented in Table 5. Namely, these are the two datasets provided in the Nokia/AAU ABG model [30] for 2 and 18 GHz, and the Qualcomm dataset for 2.9 GHz [19]. Specifically, we consider 10^3 evenly spaced points which emulated the captured real ones according to the ABG models (see Figure 2).

We first estimate its corresponding ABG coefficients from the given set of points following the steps described in Section II. As we see in Figure 2, the obtained estimation is very accurate, see Table 1 fourth and last columns for numerical values. It can be seen that the provided number of points is enough to obtain a good estimation of the ABG coefficients.

Once we have an ABG model for all the datasets, we evenly sample each ABG along its distance range, by creating sets of pairs $S_j = \{(x_i, y_i) \mid 1 \leq i \leq n_j\}$ where x_i is the distance d and y_i the path-loss predicted by the model. Observe that the number of points n_j may not be the same, consequently, weighting policies for balancing the models are necessary, as

explained in Section III-A. For the following example, the X matrix is computed as follows:

$$X = \begin{pmatrix} X_1 \\ X_2 \\ X_3 \end{pmatrix} = \begin{pmatrix} \log_{10}(109) & 1 & \log_{10}(2.9) \\ \vdots & \vdots & \vdots \\ \log_{10}(235) & 1 & \log_{10}(2.9) \\ \log_{10}(19) & 1 & \log_{10}(2.0) \\ \vdots & \vdots & \vdots \\ \log_{10}(272) & 1 & \log_{10}(2.0) \\ \log_{10}(19) & 1 & \log_{10}(18) \\ \vdots & \vdots & \vdots \\ \log_{10}(272) & 1 & \log_{10}(18) \end{pmatrix}. \quad (16)$$

Note that the WABG models the datasets with different standard deviations, and we give larger weights to those models whose standard deviation is larger, as explained in Section III-A. As a consequence, the weighting vector ω obtained expanding Equation (15) and using weighting policy 3 (see Section III-A for more detail) is presented in Equation (17).

$$\omega = M \left(\overbrace{(n_1\sigma_1^2)^{-1}, \cdots, (n_1\sigma_1^2)^{-1}}^{n_1 \text{times}}, \overbrace{(n_2\sigma_2^2)^{-1}, \cdots, (n_2\sigma_2^2)^{-1}}^{n_2 \text{times}}, \overbrace{(n_3\sigma_3^2)^{-1}, \cdots, (n_3\sigma_3^2)^{-1}}^{n_3 \text{times}} \right), \quad (17)$$

which leads to the corresponding weighting matrix presented in Equation (18), as deduced in Equation (11) and using policy 3.

$$W = \begin{pmatrix} W_1 & \cdots & 0 & \cdots & 0 \\ \vdots & \ddots & \vdots & \ddots & \vdots \\ 0 & \cdots & W_j & \cdots & 0 \\ \vdots & \ddots & \vdots & \ddots & \vdots \\ 0 & \cdots & 0 & \cdots & W_m \end{pmatrix},$$

$$W_j = M \begin{pmatrix} \frac{1}{n_j\sigma_j^2} & \cdots & 0 & \cdots & 0 \\ \vdots & \ddots & \vdots & \ddots & \vdots \\ 0 & \cdots & \frac{1}{n_j\sigma_j^2} & \cdots & 0 \\ \vdots & \ddots & \vdots & \ddots & \vdots \\ 0 & \cdots & 0 & \cdots & \frac{1}{n_j\sigma_{n_j}^2} \end{pmatrix}_{n_j \times n_j}. \quad (18)$$

Collecting all the corresponding path-loss together in a single vector Y:

$$Y = \left(y_1, \cdots, y_{n_1}, y_{n_1+1}, \cdots, y_{n_1+n_2}, y_{n_1+n_2+1}, \cdots, y_{n_1+n_2+n_3}\right)^T, \quad (19)$$

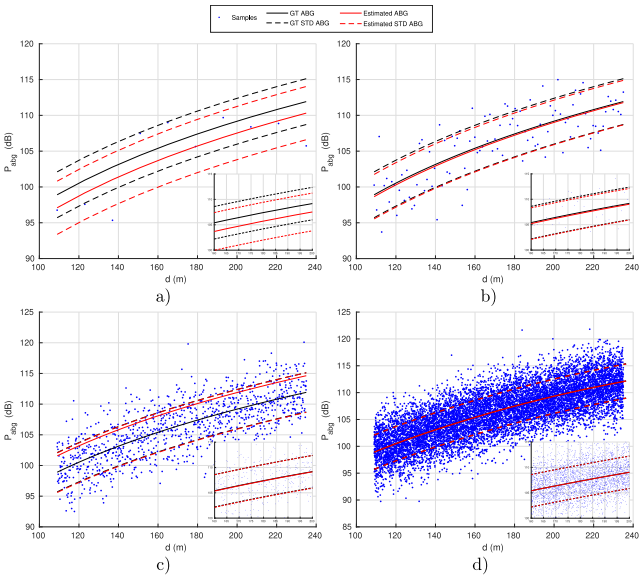

FIGURE 3. Estimation of the ABG model of the simulated UMiSC dataset (Qualcomm). Sub-figures *a), b), c)* and *d)* show evenly spaced simulated datasets with 10^1, 10^2, 10^3 and 10^4 points.

and solving Equation (9), it leads to the sought WABG coefficients for this example:

$$\begin{pmatrix} \hat{\alpha} \\ \hat{\beta} \\ \hat{\gamma} \end{pmatrix} = (X^T W X)^{-1} X^T W Y = \begin{pmatrix} 3.2 \\ 25.3 \\ 2.3 \end{pmatrix} \quad (20)$$

We compute its associated standard deviation $\sigma = 5.93$ using Equation (12). Note how the calculated value is closer to the standard deviation of Qualcomm's ABG model whose value is the smallest one. Weighting by the model's standard deviation, it leads to approaches which are close to the most accurate models, as shown in Figure 2.

The number of points of the given datasets has a strong influence on the ABG estimation. Obviously, the larger the number of points available for estimation, the more accurate is the estimation of the ABG coefficients. We show an experiment varying the number of points from 10^1 to 10^4 with an increment of 10, see Figure 3. These orders of magnitude are the most frequently found in the 5G databases. Table 1 summarizes the estimated ABG coefficients for the Qualcomm dataset, when varying the available number of points. As can be seen, the quality of the ABG model obtained is better when a larger number of points is available. Note that this is a classical result, well known in estimation theory.

B. COMPARISON AMONG DIFFERENT WEIGHTINGS SCHEMES

This experiment shows the influence of the weighting in the final WABG model. As inputs to construct the WABG model, we use three existing ABG models in the range of 2 to 18 GHz in a 5G UMiSC scenario with a NLOS environment from [19]. We extract points evenly spaced along its corresponding distance ranges and create the corresponding WABG as

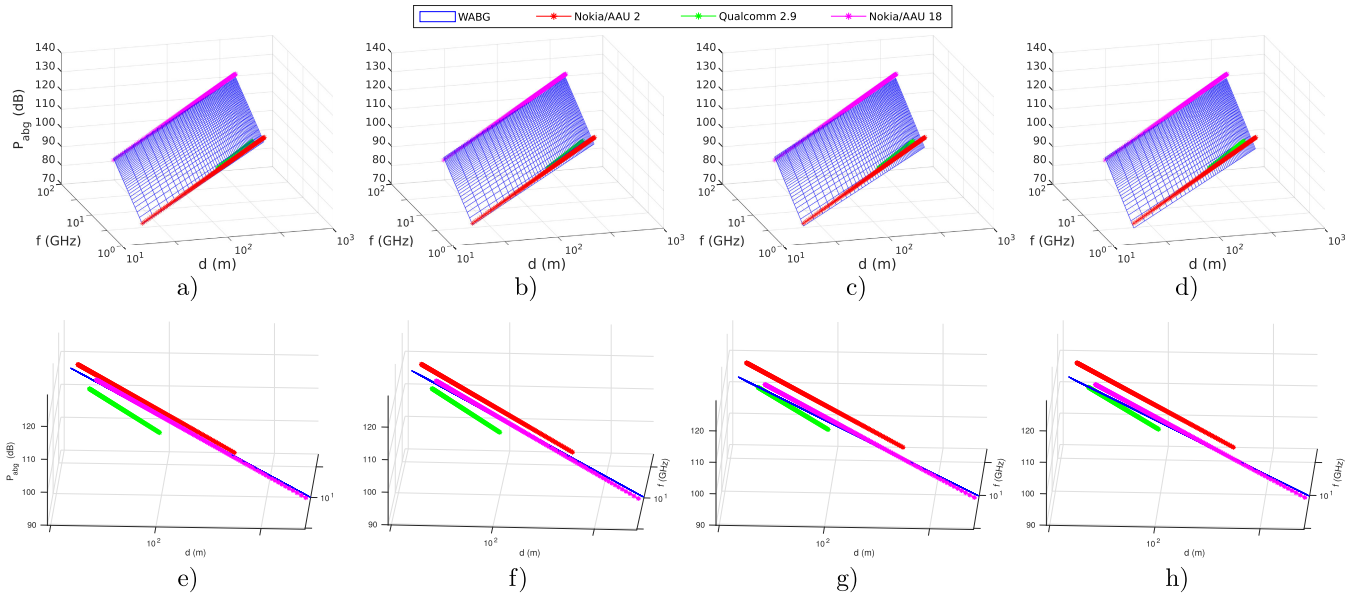

FIGURE 4. Study on the effect of different weighting schemes in the construction of WABG models. a) Basic integrated ABG model (without weighting); b) and c) WABG models in which the number of points or the individual standard deviation (respectively) are used for weighting; d) WABG model which considers both the number of points and the standard deviation of each individual model for weighting. The second row (sub-figures e) to h)) shows different views of the previous figures.

TABLE 1. Coefficients of the estimated ABG models obtained varying the number of available points. Acronym G.T. refers to the Ground Truth, the real coefficients we want to estimate using the samples.

Nº Points	10^1	10^2	10^3	10^4	G.T.
α	3.963	3.937	3.915	3.896	3.9
β	7.11	9.19	9.81	10.28	10.2
γ	2.0	2.0	2.0	2.0	2.0
σ	3.71	3.10	3.22	3.19	3.2

we did in the previous example using different weighting policies. Figure 4 shows four WABG models with different weighting policies. Figure 4.a) does not use weighting, so $W = I$, which means it is the basic integrated ABG model. Figure 4.b) and Figure 4.c) show WABG models which only use the number of points or the individual standard deviation respectively for weighting. Finally, Figure 4.d) shows a WABG model which uses the number of points and the standard deviation of each individual model to carry out the weighting process. We also provide different views of the previous figures in Figure 4.e), Figure 4.f), Figure 4.g) and Figure 4.h).

Observe in Figure 4.e) the distance between the generated ABG model (blue) and the Qualcomm dataset (green), in comparison with the WABG model (blue) in Figure 4.h). In the first one there is no weighting, and the second one is weighted both by the number of points and by the accuracy of each individual model. The difference in the number of points between the databases causes the model to move away from those models made up of fewer points, in this case, the Qualcomm dataset (green). In Figure 4.f), weighting is done by the number of points. This configuration leads to a WABG model closer to the dataset that has fewer points, that is the Qualcomm dataset (green). In Figure 4.g), weighting is done by the accuracy of each model (σ) and it leads to a fair estimation when comparing it with the ABG model (blue) in Figure 4.e).

TABLE 2. WABG coefficients obtained from the different weighting schemes and associated WABG model standard deviation (σ). Scripts F and T refer to a False or True value of weighting by number of points and standard deviation.

WABG	Number of Points - Standard Dev.			
Weighting	F-F	F-T	T-F	T-T
α	3.34	3.26	3.18	3.20
β	26.47	26.87	26.89	25.39
γ	2.03	2.11	2.23	2.29
σ	7.92	7.71	6.78	**5.89**

Table 2 shows the coefficients generated for each weighting configuration and the standard deviation of the associated WABG model (computed using Equation (7)). It can be observed that the sensitivity of the standard deviation σ when compared to the α coefficient is lower than the sensitivity of the standard deviation σ when compared to the γ coefficient. This is due to the fact that the three integrated models present quite similar behaviour along the distance, but this is not a generalized rule. Thus, the sensitivity of the standard deviation σ when compared to the α coefficient may be higher than the sensitivity of the standard deviation σ when compared to the γ coefficient, as we can see in the low band model generated for UMiOS in NLOS, see Table 6.

From now on, all the provided WABG models will be calculated considering weightings schemes by both number of points and standard deviation.

C. LOS

In order to further evaluate the performance of the proposed WABG, we create WABG models for LOS environments, in different 5G scenarios, specifically in UMiSC and UMa.

TABLE 3. Available ABG models used as WABG inputs for UMiSC and UMa 5G scenarios in LOS environment. The considered models cover different distance-frequency ranges.

Env.	Sce.	Freq. (GHz)	Reference	Organization	Dist. Range (m)	α	β (dB)	γ	σ (dB)
LOS	UMiSC	28	Sun16 [11]	NYU	27-54	1.1	46.8	2.1	4.3
		73	Sun16 [11]	NYU	27-54	1.1	46.8	2.1	4.3
		6-100	Rap17 [12]	5GCM [33]	1-121	1.9	32.9	2.1	2.0
		0.8-60	Rap17 [12]	METIS [34]	1-121	2.2	28.0	2.0	3.1
	UMa	2-38	Sun16 [11]	NYU	60-930	1.9	35.8	1.9	2.4
		6-100	Rap17 [12]	5GCM [33]	1-930	2.0	32.4	2.0	4.1

TABLE 4. Resulting WABG model for UMiSC and UMa scenario in LOS. We compare our WABG with the ABG model computed by Sun16 [19] and the 3GPP16 [3].

Env.	Sce.	Freq. Range (GHz)	Method	Dist. Range (m)	α	β (dB)	γ	σ (dB)
LOS	UMiSC	0.5-100	3GPP16 [3]	10-200	2.1	32.4	2.0	4.0
		2-73.5	Sun16 [19]	5-121	2.0	31.4	2.1	**2.9**
		0.8-100	WABG	1-121	2.0	31.1	2.1	3.2
	UMa	0.5-100	3GPP16 [3]	10-1000	2.2	28.0	42.0	4.0
		2-73.5	Sun16 [19]	58-930	2.8	11.4	42.3	4.1
		2-100	WABG	1-930	1.9	34.2	42.0	**3.1**

Table 3 shows the available ABG models for the mentioned 5G scenarios. Specifically, we have models for single frequencies, such as 28 or 73 GHz, or for several frequencies ranges, 0.8 to 60 or 6 to 100 GHz, in UMiSC scenario. In UMa, we have two ABG approaches that cover different frequency ranges. We do not have enough UMiOS path-loss models in order to create an integrate WABG with them, and then to compare it with the existent ones in the literature. Note the differences in distance ranges between UMiSC and UMa scenarios.

We use the path-loss models shown in Table 3 to create an individual WABG for each 5G scenario, following the steps given in Section III. We have a mixture of models defined for single and range frequencies.

Table 4 shows the coefficients of our WABG together with the ones given by Sun [19] and 3GPPT [3]. All the models cover a wide frequency range. The following equation has been used for specifying the maximum distance for the 3*GPP*:

$$d_{\mathrm{M}} = 4 \cdot h_{\mathrm{BS}} \cdot h_{\mathrm{UT}} \cdot \frac{f_c}{c} \tag{21}$$

In UMiSC scenario, 3GPP maximum distance d_{M} has been computed assuming a transmitter height $h_{\mathrm{BS}} = 10\,\mathrm{m}$ and a receiver height $h_{\mathrm{UT}} = 1.5$ m respectively. Carrier frequency f_c is fixed to 0.5 GHz and c is the speed of light in vacuum $3 \times 10^8\,\mathrm{ms}^{-1}$. In UMa scenario, the standard transmitter and receiver heights are fixed to 25 and 1.5 m respectively. The carrier frequency is fixed to 1 GHz. These parameters represent suitable standard conditions. However, other restrictive conditions would drive to lower maximum distances.

In UMiSC, our WABG model obtains very good accuracy, with a standard deviation of 3.2 (that is 0.3 dB below the result presented in [19], but with a wider frequency application range: between 0.5 to 100 GHz. The WABG achieves a standard deviation 1 dB smaller than the one provided by the *3GPP16* [3] with similar distance-frequency range. Observe how the maximum working range of the WABG (the maximum and minimum of the distance-frequency range) is bounded to the model ranges of the input models considered. Note that we could also expand the working range of our WABG model by integrating the 3GPP model, but in this case, it would prevent any comparison between the proposed model and the model that has been used as Ground Truth.

In UMa scenario, our WABG model obtains the best value of standard deviation, 1 dB below the one obtained by *Sun16* and 0.9 dB below the one by the *3GPP16* model. In addition, WABG covers more frequency range than that provided by *Sun16*, between 2 to 100 GHz against 2 and 73 GHz, respectively. The model in *3GPP16* expands our frequency range in low frequencies but with less accuracy.

Note that the results presented in Table 4 do not show a significant reduction of the standard deviation σ. Nevertheless, it is lower than the rest of the evaluated state-of-the-art methods, and it is remarkable how the proposed WABG model catches loss modeling from the large frequency ranges, while keeping a reduced standard deviation value.

D. NLOS

The standard deviation values observed in the LOS environment are much lower than in the counterpart NLOS. In NLOS, the fading phenomenon is more pronounced, doubling the standard deviation figures in dBs. Similar to the procedure followed for the LOS case, we provide WABG approaches from the existing ABG models for the UMiSC, UMiOS and UMa in NLOS environment. Table 5 shows the provided ABG coefficients computed from the state-of-the-art datasets in these environments [19]. We have 6, 5 and 7 different ABG models for UMiSC, UMiOS and UMa, respectively, considerably more than in LOS environment. Models are valid for single frequency located between 2 and 73.5 GHz, in

TABLE 5. ABG models in the literature for UMiSC and UMa 5G scenarios in NLOS environment obtained from Nokia/AUU database [30] and from Qualcomm, Aalto, and NYU databases [19]. The models cover different distance-frequency ranges.

Env.	Sce.	Freq. (GHz)	Company	Nº Points	Dist. Range (m)	Type	α	β (dB)	γ	σ (dB)
NLOS	UMiSC	2	Nokia/AAU	27158	19-272	M	3.5	25.0	2	7.6
		2.9	Qualcomm	34	109-235	M	3.9	10.2	2	3.2
		18	Nokia/AAU	13934	19-272	M	3.5	24.0	2	8.0
		28	NYU	20	61-186	M	2.5	51.7	2	9.7
		29	Qualcomm	34	109-235	M	4.2	11.0	2	5.3
		73.5	NYU	53	48-190	M	2.9	43.2	2	7.8
	UMiOS	2	Nokia/AAU	10377	17-138	M	4.7	−2.2	2	7.4
		2.9	Qualcomm	34	109-235	M	3.9	10.2	2	3.2
		18	Nokia/AAU	6073	23-138	M	4.9	−7.7	2	7.9
		29	Qualcomm	34	109-235	M	4.2	11.0	2	5.3
		60	Aalto	246	8-36	M	2.2	46.5	2	1.8
	UMa	2	Nokia/AAU	69542	45-1429	M, R	3.6	7.6	2	9.4
		10.25	Nokia	16743	45-1174	R	2.2	47.6	2	12.5
		18	Nokia/AAU	27154	90-1429	M	3.7	8.0	2	6.1
		28.5	Nokia	16416	45-1174	R	1.9	52.3	2	12.0
		37.625	NYU	12	61-377	M	1.0	69.4	2	9.6
		39.3	Nokia	16244	45-1174	R	1.8	53.8	2	11.6
		73.5	Nokia	15845	45-1174	R	1.9	49.7	2	10.0

TABLE 6. Low, high frequency and total WABG models in UMiSC with NLOS. We compare our WABG with the ABG computed by Sun16 [19] and 3GPP [3].

Env.	Sce.	Freq. Range (GHz)	Method	Nº Points	Dist. Range (m)	α	β (dB)	γ	σ (dB)
NLOS	UMiSC	2-18	Sun16 [19]	54350	19-272	3.5	24.4	1.9	8.0
			WABG	635	19-272	3.2	25.4	2.3	**5.9**
		28-73.5	Sun16 [19]	107	48-235	2.7	36.1	2.6	7.8
			WABG	396	48-235	2.8	35.0	2.5	**7.3**
		2-73.5	3GPP16[1] [3]	-	10-200	3.1	32.4	2.0	8.2
			Sun16 [19]	54457	19-272	3.5	24.4	1.9	8.0
			WABG	1031	19-272	3.2	24.6	2.7	**6.5**
	UMiOS	2-18	Sun16 [19]	21888	17-235	4.7	−3.1	1.8	7.6
			WABG	365	17-235	3.8	10.7	2.0	**5.2**
		29-60	Sun16 [19]	280	8-235	2.4	74.2	0.3	2.6
			WABG	156	8-235	2.3	93.4	−0.7	**2.5**
		2-60	Sun16 [19]	22168	8-235	4.4	2.4	1.9	7.8
			WABG	521	8-235	3.1	26.6	2.5	**3.8**
	UMa	2-18	Sun16 [19]	137981	45-1429	3.6	7.4	2.4	8.9
			WABG	3855	45-1429	3.4	11.1	2.3	**8.4**
		28.5-73.5	Sun16 [19]	48517	45-1174	1.9	64.6	1.2	11.2
			WABG	3707	45-1174	2.0	55.5	1.6	**10.9**
		2-73.5	3GPP16[1] [3]	-	10-1000	3.0	32.4	2.0	**8.2**
			Sun16 [19]	186498	45-1429	3.3	17.6	2.0	9.9
			WABG	7562	45-1429	2.9	31.5	1.7	9.6

case of UMiSC and UMa, and between 2 and 60 GHz, in case of UMiOS, covering different distance ranges. Observe that the initial ABG models are not defined for a single frequency range in contrast to the initial models in LOS.

Due to the large number of NLOS models found for the different scenarios (see Table 5) we develop three models for this case: a low frequency model between 2 and 18 GHz, a high frequency model between 28 and 73.5 GHz and a global model covering the entire mmWave frequency range. In case of UMiOS, the upper-bound frequency of the generated model is reduced to 60 GHz because there is not an existing approach which estimates path-losses above 60 GHz for this scenario, as shown in Table 5. The separation between low and high frequencies is not the regulated by the 5G standards. We follow the separation chosen by Sun16 model [19], in order to compare our results with that work.

Following the steps described in Section III, we compute path-loss estimations from all the provided methods varying the distances in steps of 1 m along each distance range. The resulting WABG models for low, high and the global frequency range are given in Table 6.

Focusing on UMiSC scenario, we observe that the Sun's model prioritizes the Nokia/AAU model for 2 GHz and 18 GHz against the others, see Tables 5 and 6. The number of observations of these datasets is much higher than the rest. Consequently, creating a new model which covers all the frequency range by collecting all the data together without weighting leads to unbalanced models. On the Contrary, our

[1] Actually, the 3GGP ensures a frequency range between 0.5 and 100 GHz. We establish the frequency range of the Table because of comparative reasons.

WABG model equally balances the involved ABG considering both the number of points and the standard deviation. Our WABG model reduces the standard deviation in the low, high and global path-loss models. A significant reduction is achieved in the low and global WABG models, below than 2 dB for the low frequency model and 1.1 dB for the global frequency model when compared to the results by Sun16 [19]. The proposed WABG also reduces the standard deviations in the high frequency model.

In UMiOS scenario, our WABG improves the standard deviation obtained by Sun16 for all range of frequencies: the low, high and global frequency range. WABG achieves a standard deviation for the low frequency model 5.2 dB, far from the obtained by Sun16 of 7.6 dB. The WABG model for high frequencies obtains similar standard deviation than those by Sun16 model. In the global frequency range, we also obtain the best result with a standard deviation of 3.8 dB. Note that the 3GPP does not provide any model for this scenario.

In the UMa scenario, our WABG model achieves the best standard deviation, better than that provided by Sun's model for low and high frequency ranges. However, the differences are not as severe as in the previous scenarios, below than 0.6 dB. In case of the global frequency range which cover all frequencies, the best model is the one provided by 3GPP with a standard deviation of 8.2. Our WABG ranks second, followed by Sun16 with 9.6 and 9.9 dB of standard deviation. However, note that despite obtaining worse results than 3GPP, WABG and Sun16 models cover more distance range than the former.

V. CONCLUSION

In this paper we propose a new path-loss model, the *Weighted ABG*, which allows integrating and combining different available datasets and 5G approaches for path-loss calculation. This new ABG-based model, overcomes the issues related to unbalanced data described in the literature, by using weighting policies. In addition, we have shown that the proposed WABG is able to be obtained directly from other alternative ABG models, even if no databases are available, avoiding the problem of unpublished data. We have provided the coefficients of the proposed WABG model for several 5G scenarios, including UMi and UMa, in LOS and NLOS environments.

We have carried out a complete comparison to recently published ABG models, obtaining best results with respect to the standard deviation of the studied models. Specifically, the WABG considerably overcomes the standard deviation values provided by the evaluated state-of-the-art approaches in NLOS environments and achieves comparable results in LOS.

ACKNOWLEDGMENT

Special mentions to J. Antonio Carabaña, J.L. Ruiz-Mendoza, and S. Castillo for their support and assessment. The authors would like to thank the Secretaría de Estado de Telecomunicaciones e Infraestructuras Digitales, specifically D. A. Fernández-Paniagua and P. L. Alonso for their guidance and problem definition.

REFERENCES

[1] R. Vannithamby and S. Talwar, *Towards 5G: Applications, Requirements and Candidate Technologies*. Hoboken, NJ, USA: Wiley, 2017.
[2] *IMT Vision—Framework and Overall Objectives of the Future Development of IMT for 2020 and Beyond*, document rec. ITU-R M.2083-0, Sep. 2015, pp. 1–21.
[3] *Technical Specification Group Radio Access Network; Channel Model for Frequency Spectrum Above 6 GHz*, document TR 38.900 V14.2.0, 3GPP, Dec. 2016. [Online]. Available: https://portal.3gpp.org/desktopmodules/Specifications/SpecificationDetails.aspx?specificationId=3173
[4] S. Jin, Y. Du, M. Li, Y. Huang, and X. Gao, "Pilot scheduling schemes for multi-cell massive multiple-input–multiple-output transmission," *IET Commun.*, vol. 9, no. 5, pp. 689–700, Mar. 2015.
[5] A. Tolli, L. Thiele, S. Suyama, G. Fodor, N. Rajatheva, E. De Carvalho, W. Zirwas, and J. H. Sorensen, "Massive multiple-input multiple-output (MIMO) systems," in *5G Mobile and Wireless Communications Technology*. Cambridge, U.K.: Cambridge Univ. Press, 2016.
[6] N. Rajatheva, S. Suyama, W. Zirwas, L. Thiele, G. Fodor, A. Tölli, E. Carvalho, and J. Sorensen, "Massive multiple input multiple output (MIMO) systems," in *5G Mobile and Wireless Communications Technology*. Cambridge, U.K.: Cambridge Univ. Press, 2016, ch. 2, pp. 208–247.
[7] Y. Saito, Y. Kishiyama, A. Benjebbour, T. Nakamura, A. Li, and K. Higuchi, "Non-orthogonal multiple access (NOMA) for cellular future radio access," in *Proc. IEEE 77th Veh. Technol. Conf. (VTC Spring)*, Jun. 2013, pp. 1–5.
[8] Z. Ding, M. Peng, and H. V. Poor, "Cooperative non-orthogonal multiple access in 5G systems," *IEEE Commun. Lett.*, vol. 19, no. 8, pp. 1462–1465, Aug. 2015.
[9] L. Dai, B. Wang, Y. Yuan, S. Han, C.-L. I, and Z. Wang, "Non-orthogonal multiple access for 5G: Solutions, challenges, opportunities, and future research trends," *IEEE Commun. Mag.*, vol. 53, no. 9, pp. 74–81, Sep. 2015.
[10] T. S. Rappaport, S. Sun, R. Mayzus, H. Zhao, Y. Azar, K. Wang, G. N. Wong, J. K. Schulz, M. Samimi, and F. Gutierrez, "Millimeter wave mobile communications for 5G cellular: It will work!" *IEEE Access*, vol. 1, pp. 335–349, 2013.
[11] S. Sun, T. S. Rappaport, T. A. Thomas, A. Ghosh, H. C. Nguyen, I. Z. Kovacs, I. Rodriguez, O. Koymen, and A. Partyka, "Investigation of prediction accuracy, sensitivity, and parameter stability of large-scale propagation path loss models for 5G wireless communications," *IEEE Trans. Veh. Technol.*, vol. 65, no. 5, pp. 2843–2860, May 2016.
[12] T. S. Rappaport, Y. Xing, G. R. MacCartney, A. F. Molisch, E. Mellios, and J. Zhang, "Overview of millimeter wave communications for fifth-generation (5G) wireless networks—With a focus on propagation models," *IEEE Trans. Antennas Propag.*, vol. 65, no. 12, pp. 6213–6230, Dec. 2017.
[13] N. O. Oyie and T. J. Afullo, "Measurements and analysis of large-scale path loss model at 14 and 22 GHz in indoor corridor," *IEEE Access*, vol. 6, pp. 17205–17214, 2018.
[14] M. B. Perotoni, R. D. Araujo, K. M. Santos, and D. B. Almeida, "700 MHz (4G) indoor propagation-measurement and correlation with different numerical methods," *Appl. Comput. Electromagn. Soc. J.*, vol. 35, no. 1, pp. 58–63, 2020.
[15] A. I. Sulyman, A. T. Nassar, M. K. Samimi, G. R. Maccartney, T. S. Rappaport, and A. Alsanie, "Radio propagation path loss models for 5G cellular networks in the 28 GHZ and 38 GHZ millimeter-wave bands," *IEEE Commun. Mag.*, vol. 52, no. 9, pp. 78–86, Sep. 2014.
[16] R. Hoppe, G. Wolfle, P. Futter, and J. Soler, "Wave propagation models for 5g radio coverage and channel analysis," in *Proc. 6th Asia–Pacific Conf. Antennas Propag. (APCAP)*, Oct. 2017, pp. 1–3.
[17] T. Jämsä, G. Steinböck, and M. Gustafsson, "Study of dominant path probability," in *Proc. Int. Symp. Antennas Propag. (ISAP)*, Oct. 2016, pp. 620–621.
[18] G. R. MacCartney, J. Zhang, S. Nie, and T. S. Rappaport, "Path loss models for 5G millimeter wave propagation channels in urban microcells," in *Proc. IEEE Global Commun. Conf. (GLOBECOM)*, Dec. 2013, pp. 3948–3953.
[19] S. Sun, T. S. Rappaport, S. Rangan, T. A. Thomas, A. Ghosh, I. Z. Kovacs, I. Rodriguez, O. Koymen, A. Partyka, and J. Jarvelainen, "Propagation path loss models for 5G urban micro- and macro-cellular scenarios," in *Proc. IEEE 83rd Veh. Technol. Conf. (VTC Spring)*, May 2016, pp. 1–6.

[20] T. S. Rappaport, G. R. MacCartney, M. K. Samimi, and S. Sun, "Wideband millimeter-wave propagation measurements and channel models for future wireless communication system design," *IEEE Trans. Commun.*, vol. 63, no. 9, pp. 3029–3056, Sep. 2015.
[21] R. Wahl, G. Wölfle, P. Wildbolz, and F. Landstorfer, "Dominant path prediction model for urban scenarios," in *Proc. 14th IST Mobile Wireless Commun.*, 2005, pp. 1–5.
[22] *Propagation Data and Prediction Methods for the Planning of Short-Range Outdoor Radiocommunication Systems and Radio Local Area Networks in the Frequency Range 300 MHz to 100 GHz*, document ITU-R P.1411-6-0, Feb. 2012, pp. 1–33.
[23] G. R. Maccartney, T. S. Rappaport, S. Sun, and S. Deng, "Indoor office wideband millimeter-wave propagation measurements and channel models at 28 and 73 GHz for ultra-dense 5G wireless networks," *IEEE Access*, vol. 3, pp. 2388–2424, 2015.
[24] G. R. Maccartney, T. S. Rappaport, M. K. Samimi, and S. Sun, "Millimeter-wave omnidirectional path loss data for small cell 5G channel modeling," *IEEE Access*, vol. 3, pp. 1573–1580, 2015.
[25] S. Piersanti, L. A. Annoni, and D. Cassioli, "Millimeter waves channel measurements and path loss models," in *Proc. IEEE Int. Conf. Commun. (ICC)*, Jun. 2012, pp. 4552–4556.
[26] J. B. Andersen, T. S. Rappaport, and S. Yoshida, "Propagation measurements and models for wireless communications channels," *IEEE Commun. Mag.*, vol. 33, no. 1, pp. 42–49, Jan. 1995.
[27] E. J. Violette, R. H. Espeland, R. O. DeBolt, and F. K. Schwering, "Millimeter-wave propagation at street level in an urban environment," *IEEE Trans. Geosci. Remote Sens.*, vol. 26, no. 3, pp. 368–380, May 1988.
[28] G. Lovnes, J. J. Reis, and R. H. Raekken, "Channel sounding measurements at 59 GHz in city streets," in *Proc. 5th IEEE Int. Symp. Pers., Indoor Mobile Radio Commun., Wireless Netw.-Catching Mobile Future.*, vol. 2, Sep. 1994, pp. 496–500.
[29] P. F. M. Smulders and L. M. Correia, "Characterisation of propagation in 60 GHz radio channels," *Electron. Commun. Eng. J.*, vol. 9, no. 2, pp. 73–80, Apr. 1997.
[30] M. Kyro, V. Kolmonen, and P. Vainikainen, "Experimental propagation channel characterization of mm-wave radio links in urban scenarios," *IEEE Antennas Wireless Propag. Lett.*, vol. 11, pp. 865–868, 2012.
[31] J. Meinilä, P. Kyösti, T. Jämsä, and L. Hentilä, "WINNER II channel models," in *Radio Technologies and Concepts for IMT-Advanced*. Hoboken, NJ, USA: Wiley, 2009, pp. 39–92, doi: 10.1002/9780470748077.ch3.
[32] A. C. Aitken, "IV.—On least squares and linear combination of observations," in *Proc. Roy. Soc. Edinburgh*, vol. 55. Cambridge, U.K.: Cambridge Univ. Press, 1936, pp. 42–48, doi: 10.1017/S0370164600014346.
[33] Nokia, "5G channel model for bands up to 100 GHz," White Paper, Oct. 2016. [Online]. Available: http://www.5gworkshops.com/5GCM.html
[34] V. Nurmela *et al.*, "METIS channel model, deliverable D1.4," EU Project METIS, Tech. Rep., Jul. 2015. [Online]. Available: https://metis2020.com/

DAVID CASILLAS-PEREZ received the Telecommunication Engineering degree, the master's degree in electronic control systems, and the Ph.D. degree in electronic control systems from the Universidad de Alcalá, Spain, in 2013, 2014, and 2019, respectively. He is currently a Postdoctoral Researcher with the Department of Signal Processing and Communications, Universidad de Alcalá. His research is focused on computer vision, including 3D reconstruction and machine learning techniques for mobile communication systems.

CARLOS CAMACHO-GÓMEZ was born in Zaragoza, Spain, in 1991. He received the M.S. and Ph.D. degrees in telecommunications engineering from the Universidad de Alcalá, Spain, in 2015 and 2018, respectively. He was with Universidad de Alcalà during the development of this work. Since 1st May 2020, he has been an Assistant Lecturer with the Information Systems Department, Universidad Politécnica de Madrid, Spain. He has coauthored 20 international journal articles in the field of soft computing and machine learning. His current interests deal with soft-computing techniques, hybrid algorithms, and neural networks in different applications of science and technology.

SILVIA JIMÉNEZ-FERNANDEZ was born in Madrid, Spain, in 1976. She received the B.S. and Ph.D. degrees in telecommunications engineering from the Universidad Politécnica de Madrid, Spain, in 1999 and 2009, respectively. She is currently an Associate Professor with the Department of Signal Processing and Communications, Universidad de Alcalá, Madrid, Spain, where she carries out research on the application of signal processing and machine learning techniques for mobile communication systems.

JOSE A. PORTILLA-FIGUERAS was born in Santander, Spain, in 1976. He received the B.S. and Ph.D. degrees in telecommunications engineering from the Universidad de Cantabria, Spain, in 1999 and 2004, respectively. He is currently a Full Professor with the Department of Signal Theory and Communications, and the Head of the Polytechnic School, Universidad de Alcalá, Spain. His current research interests are focused on mobile communications systems, 5G systems, and the development of machine learning algorithms.

SANCHO SALCEDO-SANZ was born in Madrid, Spain, in 1974. He received the B.S degree in physics from the Universidad Complutense de Madrid, Spain, in 1998, the Ph.D. degree in telecommunications engineering from the Universidad Carlos III de Madrid, Spain, in 2002, and the Ph.D. degree in physics from the Universidad Complutense de Madrid, in 2019. He spent one year in the School of Computer Science, The University of Birmingham, U.K, as a Postdoctoral Research Fellow. He is currently a Full Professor with the Department of Signal Processing and Communications, Universidad de Alcalá, Spain. He has coauthored more than 200 international journal articles in the field of machine learning and soft-computing. His current interests deal with soft-computing techniques, hybrid algorithms, and neural networks in different applications of science and technology.